

Chapter 7

Interfacial instabilities

This Chapter is adapted from Chapter 3 of the textbook Introduction to Hydrodynamic stability by Drazin.

In the previous Chapters we have studied instabilities arising in continuously stratified flows that have a continuous background velocity profile. However, this type of description is not adequate when trying to model the instabilities developing on an interface, such as the Rayleigh-Taylor instability created when a heavy fluid (e.g. water) lies over a lighter one (e.g. oil), or the Kelvin-Helmholz instability that occurs when two distinct fluids flow past one another. In both cases the density and/or the velocity can be discontinuous across the interface.

The study of interfacial instabilities proceeds in a similar fashion to the study of surface gravity waves in Chapter 4: the motion in the bulk of each of the two fluids is studied in addition to the motion of the interface itself.

7.1 General description of the background state

In many interfacial instability problems, we consider two fluid regions lying on top of each other, separated by an interface whose mean position at rest is $z = 0$. The top fluid has uniform density ρ_T , and a velocity in the x -direction \bar{u}_T , assumed to be constant. The bottom fluid, similarly, has a uniform density ρ_B and constant velocity \bar{u}_B in the x -direction. See Figure 7.1.

This setup is a possible steady-state of the system, as long as viscosity is ignored. We now want to determine if this steady state is stable.

7.2 General evolution equation for the perturbations

Any deviations from this steady state can induce flows in each of the two fluids, as well as motion of the interface. The total velocity of the fluid in the top region

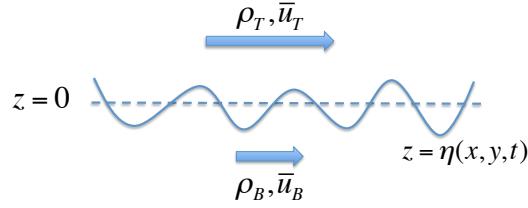


Figure 7.1: Illustration of the interfacial instability model

will therefore be $\mathbf{u}_T = \bar{\mathbf{u}}_T + \tilde{\mathbf{u}}_T$, and that in the bottom is $\mathbf{u}_B = \bar{\mathbf{u}}_B + \tilde{\mathbf{u}}_B$. We will assume, however, that the two fluids remain distinct, and that their respective densities remain constant, so there is no density perturbations. This is a valid approximation when the two fluids are immiscible for instance (ie. in the case of oil and water, or water and air to some extent, but not in the case of cream and coffee for instance).

At each point in time, the perturbed interface position can be described by the function $\eta(x, y, t)$. Fluid motions in the top region can be modeled by a function ϕ_T , such that $\tilde{\mathbf{u}}_T = \nabla\phi_T$. Similarly, fluid motion in the bottom region can be modeled with ϕ_B such that $\tilde{\mathbf{u}}_B = \nabla\phi_B$. Assuming that in both cases the initial perturbations are irrotational, they remain irrotational for all time thereafter, so that

$$\nabla^2\phi_T = 0 \text{ and } \nabla^2\phi_B = 0 \quad (7.1)$$

We will assume that perturbations are localized near the interface, so that ϕ_T tends to 0 as $z \rightarrow +\infty$, and ϕ_B tends to 0 as $z \rightarrow -\infty$. At the interface, on the other hand, we need to apply two boundary conditions. As for the case of surface gravity waves, there is a dynamic boundary condition, and a kinematic boundary condition. Let's revisit both in turn:

7.2.1 The kinematic boundary condition

The kinematic boundary condition states that the fluid at the interface must move up and down with the interface, in other words, that

$$\tilde{w} = \frac{\partial\phi}{\partial z} = \frac{D\eta}{Dt} = \frac{\partial\eta}{\partial t} + (\bar{u} + \tilde{u})\frac{\partial\eta}{\partial x} + \tilde{v}\frac{\partial\eta}{\partial y} \quad (7.2)$$

at $z = \eta$. This has to be true on both sides of the interface. Hence we get two boundary conditions at $z = \eta$,

$$\frac{\partial\phi_T}{\partial z} = \frac{\partial\eta}{\partial t} + \left(\bar{u}_T + \frac{\partial\phi_T}{\partial x}\right)\frac{\partial\eta}{\partial x} + \frac{\partial\phi_T}{\partial y}\frac{\partial\eta}{\partial y} \quad (7.3)$$

and similarly for ϕ_B . Linearizing this simply yields

$$\frac{\partial\phi_T}{\partial z} = \frac{\partial\eta}{\partial t} + \bar{u}_T\frac{\partial\eta}{\partial x} \quad (7.4)$$

and similarly for ϕ_B .

7.2.2 The dynamic boundary condition

Recall from Section 4.2 that the fluid in each of the two regions must satisfy Bernoulli's equation:

$$\frac{\partial \phi}{\partial t} + \frac{1}{2} |\mathbf{u}|^2 + \frac{p}{\rho} + gz = F(t) \quad (7.5)$$

where $F(t)$ is an arbitrary integration function of time.

Furthermore, in the absence of surface tension in the interface between the two fluids, the pressure across the interface must be continuous. This then means that

$$\begin{aligned} & \rho_T \left(\frac{\partial \phi_T}{\partial t} + \frac{1}{2} |\bar{u}_T \mathbf{e}_x + \nabla \phi_T|^2 + g\eta - F_T(t) \right) \\ &= \rho_B \left(\frac{\partial \phi_B}{\partial t} + \frac{1}{2} |\bar{u}_B \mathbf{e}_x + \nabla \phi_B|^2 + g\eta - F_B(t) \right) \end{aligned} \quad (7.6)$$

This equation must hold for the steady state background solution (for which $\eta = 0$ and $\tilde{\phi} = 0$). This implies that

$$\rho_T \left(\frac{1}{2} \bar{u}_T^2 - F_T(t) \right) = \rho_B \left(\frac{1}{2} \bar{u}_B^2 - F_B(t) \right) \quad (7.7)$$

This provides a relationship between $F_T(t)$ and $F_B(t)$.

Subtracting the background equation, and linearizing the remainder, we then get

$$\rho_T \left(\frac{\partial \phi_T}{\partial t} + \bar{u}_T \frac{\partial \phi_T}{\partial x} + g\eta \right) = \rho_B \left(\frac{\partial \phi_B}{\partial t} + \bar{u}_B \frac{\partial \phi_B}{\partial x} + g\eta \right) \quad (7.8)$$

Finally, note that while both the dynamic and kinematic boundary conditions should be applied at $z = \eta$, by Taylor-expansion around $z = 0$ it is easy to show that they can equivalently be applied at $z = 0$, to linear order. In summary, we have to solve

$$\nabla^2 \phi_T = 0 \text{ and } \nabla^2 \phi_B = 0 \quad (7.9)$$

subject to boundary conditions $\phi_T \rightarrow 0$ as $z \rightarrow +\infty$, $\phi_B \rightarrow 0$ as $z \rightarrow -\infty$, and

$$\begin{aligned} \frac{\partial \phi_T}{\partial z} &= \frac{\partial \eta}{\partial t} + \bar{u}_T \frac{\partial \eta}{\partial x} \\ \frac{\partial \phi_B}{\partial z} &= \frac{\partial \eta}{\partial t} + \bar{u}_B \frac{\partial \eta}{\partial x} \\ \rho_T \left(\frac{\partial \phi_T}{\partial t} + \bar{u}_T \frac{\partial \phi_T}{\partial x} + g\eta \right) &= \rho_B \left(\frac{\partial \phi_B}{\partial t} + \bar{u}_B \frac{\partial \phi_B}{\partial x} + g\eta \right) \end{aligned} \quad (7.10)$$

at $z = 0$.

7.3 General Solution

Noting that all of the coefficients of the governing equations and respective boundary conditions are independent of time and of x and y , we can assume that

$$\phi_T = \hat{\phi}_T(z)e^{ik_x x + ik_y y + \lambda t} \quad (7.11)$$

and similarly for ϕ_B , as well as

$$\eta = \hat{\eta}e^{ik_x x + ik_y y + \lambda t} \quad (7.12)$$

From the two irrotationality conditions, and the boundary conditions at $z \rightarrow \pm\infty$, we get that

$$\begin{aligned} \hat{\phi}_T(z) &= \hat{\phi}_+ e^{-kz} \\ \hat{\phi}_B(z) &= \hat{\phi}_- e^{kz} \end{aligned} \quad (7.13)$$

where $k^2 = k_x^2 + k_y^2$. Plugging this into the kinematic and dynamic boundary conditions, we then get

$$\begin{aligned} -k\hat{\phi}_+ &= \lambda\hat{\eta} + ik_x \bar{u}_T \hat{\eta} \\ k\hat{\phi}_- &= \lambda\hat{\eta} + ik_x \bar{u}_B \hat{\eta} \\ \rho_T (\lambda\hat{\phi}_+ + ik_x \bar{u}_T \hat{\phi}_+ + g\hat{\eta}) &= \rho_B (\lambda\hat{\phi}_- + ik_x \bar{u}_B \hat{\phi}_- + g\hat{\eta}) \end{aligned} \quad (7.14)$$

which is an algebraic homogeneous system of 3 equations for 3 unknowns, $\hat{\phi}_+$, $\hat{\phi}_-$ and $\hat{\eta}$. Solving for $\hat{\phi}_+$ and $\hat{\phi}_-$ in terms of $\hat{\eta}$, we first get

$$\begin{aligned} \hat{\phi}_+ &= -(\lambda + ik_x \bar{u}_T) \frac{\hat{\eta}}{k} \\ \hat{\phi}_- &= (\lambda + ik_x \bar{u}_B) \frac{\hat{\eta}}{k} \end{aligned} \quad (7.15)$$

Plugging this into the dynamic boundary condition, we then get

$$\rho_T (-(\lambda + ik_x \bar{u}_T)^2 + gk) = \rho_B ((\lambda + ik_x \bar{u}_B)^2 + gk) \quad (7.16)$$

Finally, letting $\lambda = -ik_x c$ as usual, we get

$$\rho_T (k_x^2 (\bar{u}_T - c)^2 + gk) = \rho_B (-k_x^2 (\bar{u}_B - c)^2 + gk) \quad (7.17)$$

This is a quadratic equation for c .

$$(\rho_T + \rho_B)c^2 - 2(\bar{u}_T \rho_T + \bar{u}_B \rho_B)c + (\rho_T \bar{u}_T^2 + \rho_B \bar{u}_B^2) + (\rho_T - \rho_B) \frac{gk}{k_x^2} = 0 \quad (7.18)$$

whose solutions are

$$c = \frac{(\bar{u}_T \rho_T + \bar{u}_B \rho_B) \pm \sqrt{(\bar{u}_T \rho_T + \bar{u}_B \rho_B)^2 - (\rho_T + \rho_B) \left[(\rho_T \bar{u}_T^2 + \rho_B \bar{u}_B^2) + (\rho_T - \rho_B) \frac{g}{k_x} \right]}}{\rho_T + \rho_B} \quad (7.19)$$

which simplifies into

$$c = \frac{(\bar{u}_T \rho_T + \bar{u}_B \rho_B) \pm \sqrt{-\rho_T \rho_B (\bar{u}_T - \bar{u}_B)^2 - (\rho_T^2 - \rho_B^2) \frac{gk}{k_x^2}}}{\rho_T + \rho_B} \quad (7.20)$$

This expression shows that unstable modes (with $\Im(c) > 0$) exist only if the term under the square root is negative, and if they do, then there is always one growing mode for each decaying one, and vice versa. The condition for the existence of unstable modes can be recast in the form

$$\rho_T \rho_B (\bar{u}_T - \bar{u}_B)^2 > (\rho_B^2 - \rho_T^2) \frac{gk}{k_x^2} \quad (7.21)$$

This shows that

- if $\rho_B \leq \rho_T$, then the system is always unstable. This is not surprising, as it would mean that the top fluid is denser than the bottom one, a situation that is intrinsically unstable even in the absence of shear (see below for more detail).
- if $\rho_B > \rho_T$, then, for a given shearing rate, there is always a critical wavenumber k_x above which the system is unstable, and below which the system is stable. In other words, shear instabilities can always develop on a stably stratified interface, as long as their wavelength is small enough.

7.4 Special limits

Various interesting special limits of the study made above exist.

7.4.1 The Kelvin-Helmholtz instability

The Kelvin-Helmholtz instability is described by the formalism above in the limit where $\rho_T = \rho_B$. In that case, as we just saw, the system is always unstable for all values of k_x , and with

$$c = \frac{(\bar{u}_T + \bar{u}_B) \pm i|\bar{u}_T - \bar{u}_B|}{2} \quad (7.22)$$

we find that the growth rate λ of the modes is

$$\lambda = \frac{\pm k_x |\bar{u}_T - \bar{u}_B| - ik_x (\bar{u}_T + \bar{u}_B)}{2} \quad (7.23)$$

This has a somewhat unphysical ultraviolet catastrophe, in the sense that modes with larger k_x always have larger growth rates, regardless of k_x . In reality, modes with very large k_x are subject to either to viscosity or surface tension, both of which can suppress the instability.

The nonlinear development of the Kelvin-Helmholtz instability leads to the roll-up of the disturbances, and to spectacular spiral patterns that can be observed most easily in the laboratory, but also sometimes in cloud patterns when the conditions are just right.

7.4.2 Internal interfacial gravity waves

Internal interfacial gravity waves are gravity waves that ride on an interface between two fluids as described above, with $\rho_B > \rho_T$ and no background shear. They have

$$c = \pm \frac{\sqrt{(\rho_B^2 - \rho_T^2) \frac{gk}{k_x^2}}}{\rho_T + \rho_B} \quad (7.24)$$

which leads to an oscillation frequency

$$\omega = \Re(-ik_x c) = \pm \sqrt{\frac{\rho_B - \rho_T}{\rho_T + \rho_B} gk} \quad (7.25)$$

For 1D waves (assuming $k_y = 0$), this is often re-written as

$$\omega = \pm \sqrt{\tilde{g}k} \quad (7.26)$$

where

$$\tilde{g} = \frac{\rho_B - \rho_T}{\rho_T + \rho_B} \quad (7.27)$$

is called the *reduced gravity*. This shows that gravity waves riding on the interface between two fluids whose densities are not very different oscillate *very* slowly. This can be demonstrated in the lab quite easily, and looks really remarkable – the waves sometimes move so slowly that they appear frozen in time.

7.4.3 The Rayleigh-Taylor instability

In the opposite limit where the two fluids are such that $\rho_B < \rho_T$, or in the more unusual (but not impossible) case where gravity changes sign, then the background is always unstable even in the absence of shear. Perturbations have

$$c = \frac{\pm i \sqrt{(\rho_T^2 - \rho_B^2) \frac{gk}{k_x^2}}}{\rho_T + \rho_B} \quad (7.28)$$

so that (for 1D perturbations for instance)

$$\lambda = \pm \sqrt{\tilde{g}k_x} \quad (7.29)$$

Again, this instability suffers from an ultraviolet catastrophe, that can be resolved as in the case of the Kelvin-Helmholtz instability by remembering that viscosity or surface tension can stabilize large-wavenumber modes.

The nonlinear development of the Rayleigh-Taylor instability leads to the formation of spectacular mushroom-like plumes.